JGR Space Physics

RESEARCH ARTICLE
10.1029/2022JA030804

Key Points:

- Using 7-year Van Allen Probe-A data, we have statistically studied oblique whistler-mode waves in the Earth's magnetosphere
- Most of oblique waves are poleward propagating and their favored magnetic latitudes increase with magnetic local time, supporting propagation effect as the main cause
- There also exist some equatorward propagating oblique waves confined within 5° in the midnight sector, which may be locally excited

Correspondence to:

X. Gao and Q. Lu,
gaox1@mail.ustc.edu.cn;
qmlu@ustc.edu.cn

Citation:

Gao, X., Lu, Q., Kang, N., Ke, Y., Ma, J., Tsurutani, B., et al. (2022). Study on source region and generation mechanism of oblique whistler-mode waves in the Earth's magnetosphere. *Journal of Geophysical Research: Space Physics*, *127*, e2022JA030804. https://doi.org/10.1029/2022JA030804

Received 17 JUL 2022
Accepted 30 AUG 2022

Study on Source Region and Generation Mechanism of Oblique Whistler-Mode Waves in the Earth's Magnetosphere

Xinliang Gao[1,2,3], Quanming Lu[1,2,3], Ning Kang[4], Yangguang Ke[1,2], Jiuqi Ma[1,2], Bruce Tsurutani[5], Rui Chen[1,2], and Huayue Chen[1,2]

[1]Deep Space Exploration Laboratory, School of Earth and Space Sciences, University of Science and Technology of China, Hefei, China, [2]CAS Center for Excellence in Comparative Planetology, CAS Key Laboratory of Geospace Environment, Hefei, China, [3]Collaborative Innovation Center of Astronautical Science and Technology, Harbin, China, [4]Department of Atmospheric and Oceanic Sciences, University of California, Los Angeles, CA, USA, [5]Retired, Pasadena, CA, USA

Abstract Oblique whistler-mode waves are as important as quasi-parallel waves in regulating electron dynamics in radiation belts. However, their generation mechanism and corresponding source region are still under debate. By analyzing nearly 7-year Van Allen Probe-A data, we have thoroughly investigated lower-band ($<0.5f_{ce}$) and upper-band ($>0.5f_{ce}$) oblique whistler-mode waves in the Earth's inner magnetosphere. We found the majority of poleward propagating oblique waves preferentially occur at relatively larger magnetic latitudes (MLATs), and their favored MLATs are strongly dependent on magnetic local time. Combined with ray tracing simulation results, it is proposed that parallel waves generated at the equator propagate toward poles and turn oblique to the ambient magnetic field, leading to oblique waves detected at large |MLAT|. This propagation effect is the main cause of oblique whistler-mode waves in the Earth's magnetosphere. There also exist some equatorward propagating oblique waves, which are mainly confined within ± 5° around midnight and considered to be locally excited. Our study provides a comprehensive understanding of the generation and distribution of oblique whistler-mode waves in the Earth's magnetosphere.

Plain Language Summary Quai-parallel whistler-mode waves have attracted more attention than oblique whistler-mode waves in the community, since oblique waves typically have the smaller magnetic amplitude in the Earth's magnetosphere. However, based on Cluster data, Artemyev, Agapitov, et al. (2015), https://doi.org/10.1038/ncomms8143 suggested that oblique whistler-mode waves may carry up even more wave energy involved in wave-particle resonant interactions. Therefore, we have thoroughly studied those oblique waves by analyzing 7-year Van Allen Probe-A wave spectrum data, especially focusing on the source region and physical causes. Actually, there already exist two principal candidates in the literature: propagation effects and local generation. Our statistical results show that most of oblique whistler-mode waves are poleward propagating, which preferentially occur at relatively larger latitudes and show strong dependence on magnetic local time. Our ray tracing results are consistent with observations, suggesting the propagation effect is the dominant generation mechanism in the Earth's magnetosphere. We also find some local excitation effects, but only for equatorward propagating oblique waves near the equator in the midnight sector.

1. Introduction

Whistler-mode waves are very common electromagnetic emissions falling within the frequency range of 0.1–0.8 f_{ce} (where f_{ce} is the equatorial electron gyrofrequency) in the Earth's magnetosphere. They are also known as chorus waves, appearing as a series of repetitive coherent emissions (Gao et al., 2022; Lu et al., 2021). There usually exists a power gap around $0.5f_{ce}$ in the spectrum, dividing the spectrum into lower and upper bands (Gao et al., 2014, 2019; Li et al., 2019; Santolik et al., 2003; Tsurutani & Smith, 1974, 1977; Yagitani et al., 2014). They have attracted more and more attention due to their important role in accelerating seed electrons (~100 keV) to relativistic energies (>1 MeV) and scattering low-energy (0.1–30 keV) electrons to precipitate into the upper atmosphere (Horne et al., 2005; Liu et al., 2015, 2020; Lorentzen et al., 2001; Ni et al., 2008; Thorne et al., 2010, 2013; Tsurutani et al., 2013; Xiao et al., 2009, 2015). The efficiency of interactions between whistler-mode waves and electrons is strongly determined by wave properties, and one of them is the wave normal angle (WNA; Ni et al., 2011; Shprits & Ni, 2009; Verkhoglyadova et al., 2010). In the Earth's magnetosphere, both quasi-parallel (WNA< 45°) (Burton & Holzer, 1974; Goldstein & Tsurutani, 1984; Li et al., 2011, 2013; Tsurutani et al., 2020) and oblique (WNA > 45°) (Agapitov et al., 2013; Gao et al., 2016; Li et al., 2011, 2013;

Liu et al., 2021; Mourenas et al., 2014) whistler-mode waves have been widely observed. Although quasi-parallel whistler-mode waves typically have the much larger magnetic amplitudes (Li et al., 2011), previous studies pointed out oblique whistler-mode waves play a crucial role in electron dynamics as well as quasi-parallel waves (Artemyev, Agapitov, et al., 2015, 2016; Li et al., 2014; Mourenas et al., 2012). For example, based on Cluster data, Artemyev, Agapitov, et al. (2015) proposed that oblique whistler-mode waves may carry up even more wave energy involved in wave-particle resonant interactions.

However, the source region and generation mechanism of oblique whistler-mode waves are still under debate. Generally, there are two major potential generation mechanisms of oblique whistler-mode waves in the literature (Artemyev et al., 2016; Chen et al., 2013; Gao et al., 2016; Ke et al., 2017; Li, Mourenas, et al., 2016; Lu et al., 2019; Mourenas et al., 2015; Zhou et al., 2019). Both theoretical and simulation results showed that whistler-mode waves are initially excited by anisotropic energetic (~10s keV) electrons with small WNAs near the magnetic equator (Nunn, 1971; Omura et al., 2008; Santolik et al., 2014; Tsurutani et al., 1979; Tsurutani & Smith, 1977), and then propagate toward higher latitudes and the wave vector gradually turns oblique mainly due to the inhomogeneity of background magnetic field (Chen et al., 2013; Ke et al., 2017; LeDocq et al., 1998; Lu et al., 2019; Taubenschuss et al., 2016). In this scenario, oblique whistler-mode waves are caused by the propagation effect and preferentially occur at higher latitudes with the propagating direction toward the poles (Agapitov et al., 2013; Haque et al., 2010; Li et al., 2013). Besides, oblique whistler-mode waves may be locally excited by anisotropic energetic electrons if there simultaneously exists a beam-like/plateau population around the phase velocity of wave in the parallel velocity distribution of electrons (Artemyev et al., 2016; Gao et al., 2016; Li, Mourenas, et al., 2016; Mourenas et al., 2015). This beam-like population may either suppress the severe Landau damping of oblique whistler-mode waves or directly provide the free energy to excite oblique waves. Therefore, these waves can have the equatorward propagating direction, besides the poleward direction (Li et al., 2013; Taubenschuss et al., 2016).

In this paper, using nearly 7-year (August 2012–December 2018) of Van Allen Probe-A plasma wave data, we present a statistical analysis of lower-band ($<0.5f_{ce}$) and upper-band ($>0.5f_{ce}$) oblique whistler-mode waves in the Earth's magnetosphere. We clearly find there are two main populations with different favored latitudes, and the dependences of their favored latitudes on magnetic local time (MLT) are quite distinct. The statistical results are also compared with the ray tracing results. Our study provides direct observational support for the generation mechanism and corresponding source region of oblique whistler-mode waves in the Earth's magnetosphere.

2. Data Sources and Ray Tracing Method

The Van Allen Probes, including two identical probes (A and B), are orbiting around the Earth with the perigee of ~$1.1R_E$ (radius of the Earth), apogee of ~$5.8R_E$, and inclination of 10° (Kessel et al., 2013; Mauk et al., 2013). This mission was launched on 30 August 2012, and both probes are equipped with the Electric and Magnetic Field Instrument Suite and Integrated Science (EMFISIS) suite which provides vastly improved measurement of whistler-mode chorus waves in the inner magnetosphere (Kletzing et al., 2013). In this study, we have collected the survey mode data from the waveform receiver (WFR) of EMFISIS from August 2012 to December 2018. The survey mode data provide the wave power spectrum ranging from 10 Hz to 12 kHz and a complete spectrum matrix every 6 s. The spectral matrices data set has been processed in the field-aligned coordinate system to get polarization parameters of whistler-mode waves. The tri-axial fluxgate magnetometer (MAG) is used to obtain the local electron cyclotron frequencies (Kletzing et al., 2013). The AE index is obtained from OMNI website with 1-min resolution, which is used to estimate the plasmapause position (O'Brien & Moldwin, 2003).

To investigate the propagation of whistler-mode waves in the Earth's magnetosphere, a ray tracing program is implemented by solving Hamilton's equations (Haselgrove, 1955; Kimura, 1966). In this program, the linear dispersion relation in cold plasma is used for whistler-mode waves. The background magnetic field is obtained from the T89 model (Tsyganenko, 1989), where the field configuration depends on the geomagnetic Kp index. The background plasma density follows an empirical model, which is incorporated by the equatorial density model (Carpenter & Anderson, 1992) and a field-aligned density model (Chen et al., 2012; Denton et al., 2002).

3. Observation Results

Figure 1 presents the power spectrum measurement during nearly one orbit of Van Allen Probe-A, including (a) the magnetic spectrum, (b) electric spectrum, (c) ellipticity, (d) WNA, and (c) P_f flag, respectively. In each panel,

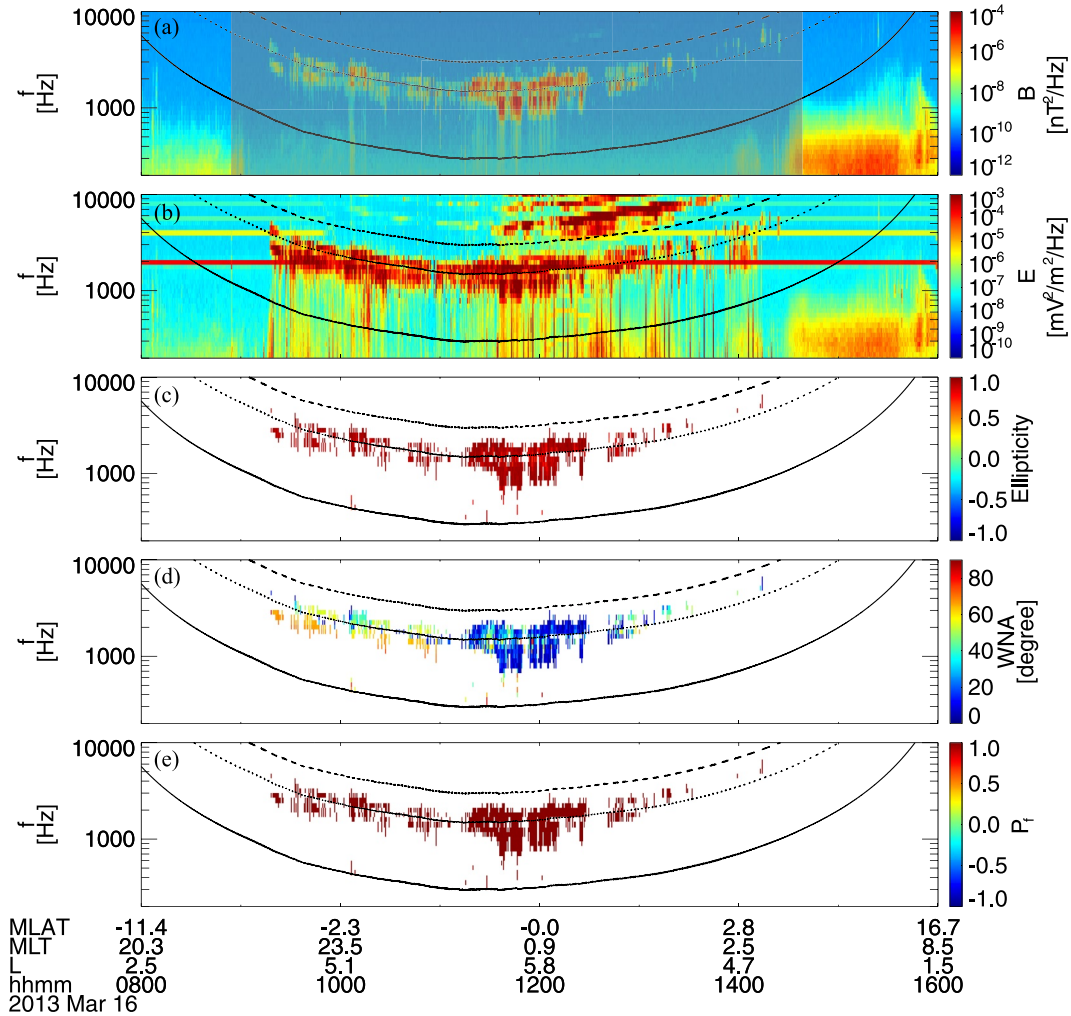

Figure 1. An overview of power spectrum measurement during nearly one orbit of Van Allen Probe-A, including (a) the magnetic spectrum, (b) electric spectrum, (c) ellipticity, (d) wave normal angle, and (c) P_f flag, respectively. In each panel, the black solid, dotted, and dashed lines denote the frequencies of 0.1, 0.5, and 1 f_{ce}, respectively. The shaded region in panel a is outside the plasmapause.

the black solid, dotted, and dashed lines denote the frequencies of 0.1, 0.5, and 1 f_{ce}, respectively. To exclude plasmaspheric hiss (Zhou et al., 2016), we only consider whistler-mode waves outside the plasmapause, which is shaded in gray in Figure 1a. The P_f flag (−1 or 1) denotes the propagating direction of waves: −1 for the equatorward propagating direction and 1 for the poleward propagating direction (also done in Gao et al., 2017). At each time point, that is, every 6 s, we checked every frequency bin between 0.1 and 1 f_{ce}, and recorded the data point only if the corresponding magnetic power was $>10^{-8}$ nT^2/Hz and ellipticity was >0.7 (nearly right-handed circularly polarized; Verkhoglyadova et al., 2010). The data points satisfying the above criteria have been shown in Figures 1c–1e. Then, according to the WNA shown in Figure 1d, we further classify these data points into quasi-parallel whistler-mode waves (WNA < 45°) and oblique waves (WNA > 45°). It is worth noting that the Gendrin angle may be a natural delimitation between quasi-parallel and oblique waves (Agapitov et al., 2018; Albert, 2017; Li, Santolik, et al., 2016), but the 45° is chosen here for convenience in both selecting events and further comparing ray tracing simulations with observations. Finally, we have collected over 6 million data points for oblique whistler-mode waves during August 2012 and December 2018 using Van Allen Probe-A data.

The measurement coverage of Van Allen Probe-A is presented in Figures 2a and 2d, where bins with less than 600 time points, that is, 1 hr, have been discarded. The satellite provides good coverage over all MLTs and between the L-shells of 3–6.5 (Figure 2a). Due to the low inclination of satellite, measurements are limited to magnetic latitudes (MLATs) of ± 20° (Figure 2d). Figures 2b and 2e display the occurrence rate of lower-band oblique

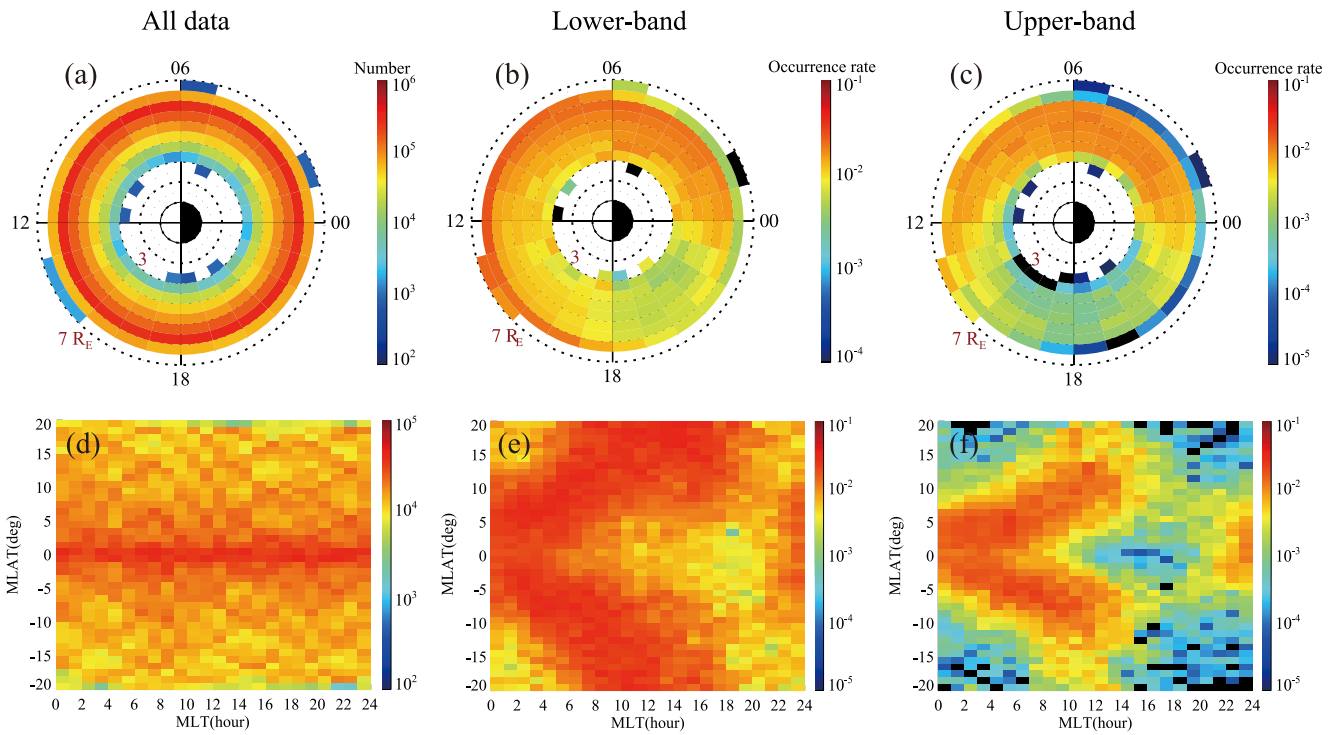

Figure 2. The measurement coverage of Van Allen Probe-A in the (a) L-magnetic local time (L-MLT) and (d) magnetic latitude-magnetic local time (MLAT-MLT) planes. The occurrence rate of lower-band oblique whistler-mode waves in the (b) L-MLT and (e) MLAT-MLT planes, respectively. Panels c and f show the occurrence of upper-band oblique whistler-mode waves in the same format. The bin size in top row and bottom row is $0.5R_E \times 1$ hr (R_E is the Earth's radius) and $1° \times 1$ hr, respectively.

whistler-mode waves in the L-MLT and MLAT-MLT planes, respectively. Here the occurrence rate in each bin is defined by the ratio between the number of time points of oblique whistler-mode waves and satellite measurements. Note that there may be more than one data points (with different frequencies) selected at the same time point, so we only count once for such data points to avoid duplicated counting.

In Figure 2b, it is found lower-band oblique whistler-mode waves can occur from the midnight to dusk sector, but they are generally found at larger L-shells on dayside. Interestingly, the oblique chorus MLAT dependence gradually increases with increasing MLT (i.e., from midnight to noon; Figure 2e). Specifically, the favored latitude of lower-band oblique waves reaches up to $\pm 20°$ (and possibly beyond) at noon but is limited to $\pm 10°$ at midnight. The distribution of upper-band oblique waves is shown in Figures 2c and 2f. Upper-band oblique waves preferentially occur in the dawn sector (Figure 2c). Oblique chorus has low occurrence rates from the noon to dusk sector. The strong dependence of oblique chorus' predominant latitudes on MLT is also found in Figure 2f but within a narrower range of latitude. There is a sharp drop in the occurrence rate at $\pm 5°$ (or $\pm 10°$) at midnight (or noon).

Using the wave propagating direction (i.e., the P_f), we further divide the oblique waves into two categories, such as poleward ($P_f = 1$) and equatorward ($P_f = -1$). Based on previous simulation and observation works, whistler-mode waves with the equatorward propagating direction are generally considered to be locally excited within the source region (Ke et al., 2017; Li et al., 2013; Taubenschuss et al., 2016). Figures 3a and 3b display the distribution of equatorward propagating oblique waves, while Figures 3c and 3d present the distribution of poleward propagating oblique waves. The equatorward propagating oblique waves are mainly distributed near the magnetic equator in the midnight sector (22–6 hr), suggesting oblique whistler-mode waves can be locally excited near the magnetic equator (source region). But their occurrence rate is much lower than poleward propagating oblique waves. Just as expected, poleward propagating oblique waves preferentially appear at higher latitudes, and there is a clear drop of occurrence rate at the equator. Moreover, there also exists the remarkable dependence of favored MLATs on MLT similar to that in Figures 2e and 2f.

For comparison, we also present the distribution of quasi-parallel whistler-mode waves in Figure 4 following the same format as Figure 3. Unlike lower-band oblique waves, the quasi-parallel waves with the equatorward

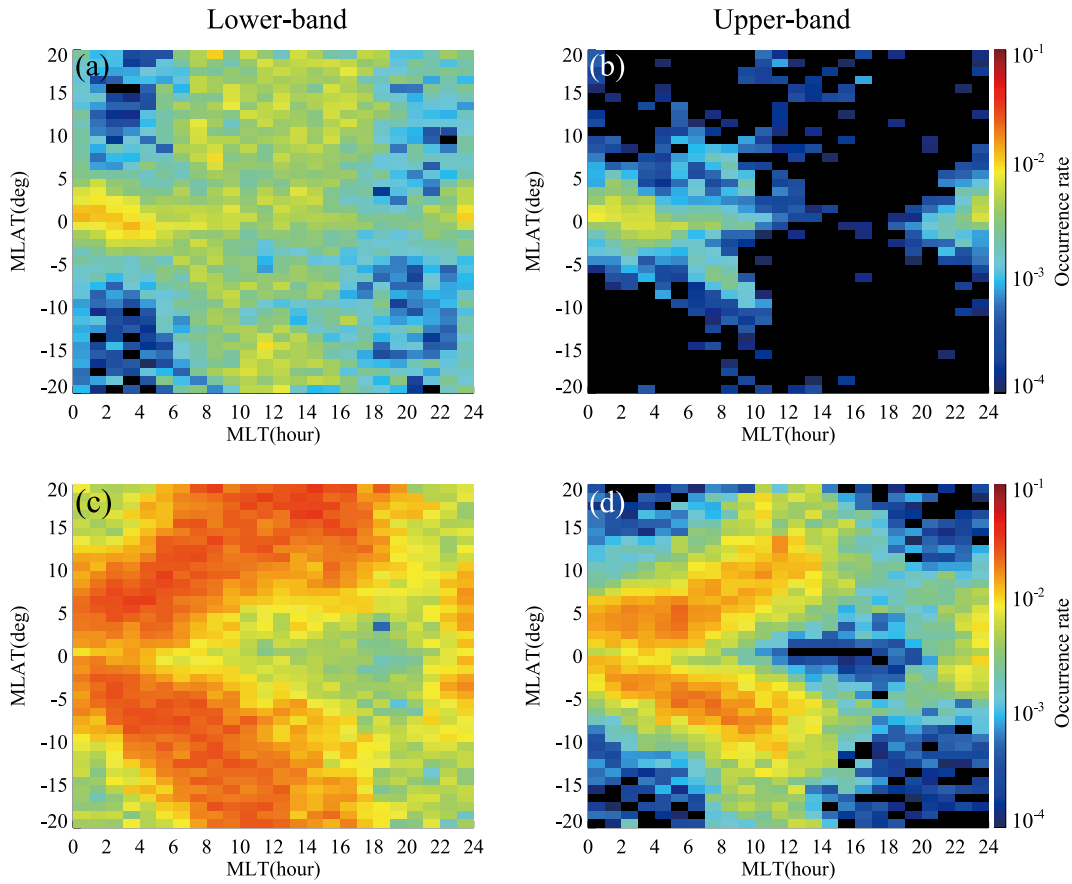

Figure 3. The occurrence rate of equatorward propagating (a) lower-band and (b) upper-band oblique waves in the magnetic latitude-magnetic local time (MLAT-MLT) plane. The occurrence rate of pole propagating (c) lower-band and (d) upper-band oblique waves in the MLAT-MLT plane.

propagating direction preferentially occur on the dayside over a broad range of MLATs (Figure 4a), that is, from −20° to 20°. Similarly, the poleward propagating quasi-parallel waves also usually appear on the dayside (Figure 4c), which is quite different with that shown in Figure 3c. The equatorward propagating upper-band quasi-parallel waves mainly occur on the nightside (Figure 4b), similar to that shown in Figure 3b, but the poleward propagating upper-band quasi-parallel waves favor the lower MLATs than upper-band oblique waves (Figure 4d). If not separating oblique and quasi-parallel waves, the clear dependence of favored MLATs on MLT will become blurred due to their quite different distributions.

Here we propose that the generation and corresponding distribution of poleward propagating oblique waves shown in Figures 3c and 3d are caused by the propagation effect. The ray tracing method has been widely used to study the wave propagation (Breuillard et al., 2012, 2015; Chen et al., 2013), and we use this method to explain the observed MLT dependence of the favored MLATs of poleward propagating oblique waves. In our simulations, the background magnetic field is obtained from the T89 model for simplicity, and we fix the Kp index as 4 to represent a geoactive period. The whistler-mode wave is launched at the magnetic equator at $L = 6$ over different MLTs. The plasmapause is estimated at $L = 3.76$, which is far away from the launching waves. The frequency of whistler-mode wave ranges from 0.1 to 0.8 f_{ce}, and its initial WNA is set as 0°. As an example, Figures 5a and 5b present the simulation results at the midnight (MLT = 0 hr). As expected, the background magnetic field is stretched from the standard dipole field in Figure 5a. After the parallel whistler-mode waves are launched, they propagate toward the higher latitudes and turn oblique. In Figure 5b, we have marked the threshold latitude where the WNA of each wave becomes larger than 45° for the first time. The higher-frequency wave becomes oblique, that is, WNA > 45°, at the smaller latitude. We also present the observed favored latitudes of poleward propagating lower-band and upper-band oblique waves as a function of MLT in Figures 5c and 5d, respectively, where the gray diamonds denote the median value with the first and third quartiles as error bars. Here all selected

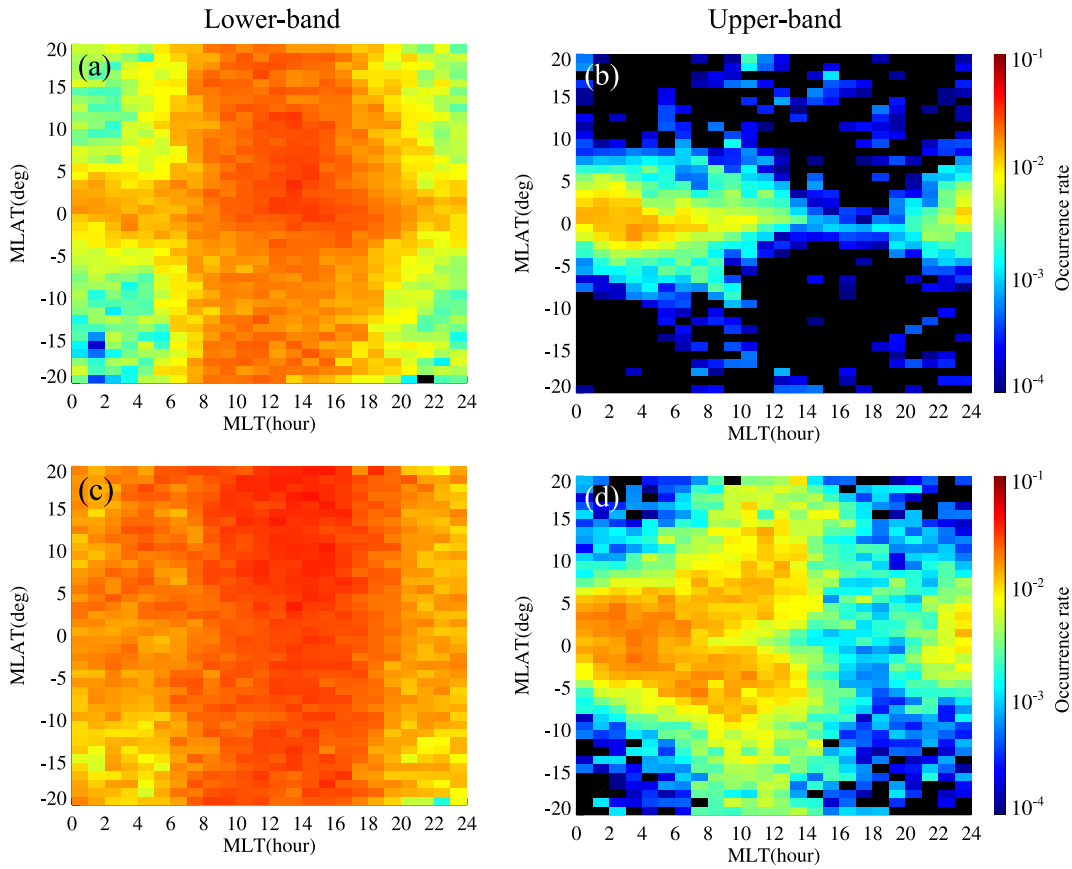

Figure 4. The distribution of quasi-parallel whistler-mode waves with the same format as Figure 3.

data points (including those chosen at the same time point) are involved. For comparison, the threshold latitudes of lower-band and upper-band waves at different MLTs, obtained from ray tracing simulations, are also plotted in Figures 5c and 5b, respectively. For both lower-band and upper-band oblique whistler waves, the favored latitude of poleward propagating waves generally increases with the MLT (i.e., from 0 to 12 hr). The unexpected drop at MLT = 10 hr in Figure 5c should be caused by the limited latitude of Van Allen Probe-A. The threshold latitudes of each whistler mode also present a quite similar trend with the increasing MLT, which is due to the decreasing inhomogeneity of background magnetic field from midnight to noon. There is a good agreement between the observations and ray tracing simulations, so it is reasonable to draw the conclusion that the poleward propagating oblique whistler-mode waves are mainly a result from wave propagation.

4. Summary and Discussion

In this study, we have thoroughly investigated lower-band ($<0.5f_{ce}$) and upper-band ($>0.5f_{ce}$) oblique whistler-mode waves in the Earth's magnetosphere by analyzing nearly 7-year (August 2012–December 2018) Van Allen Probe-A data. We find poleward propagating oblique whistler-mode waves preferentially occur at relatively larger latitudes, and their occurrence latitudes increase with increasing MLT. Upper-band oblique waves are typically observed at lower latitudes than lower-band waves in the same MLT. The ray tracing simulations are in agreement with the observations. Therefore, we propose that obliquely propagating chorus waves are caused by the propagation effect, and the strong MLT dependence of their favored latitudes is due to the different inhomogeneity of background magnetic field over MLT. There also exist some equatorward propagating oblique waves, which are mainly confined within ± 5° in the midnight sector. These waves are considered to be locally excited. Since the poleward propagating waves have much larger occurrence rates, propagation effects are believed to be the dominant generation mechanism of oblique whistler-mode waves in the Earth's magnetosphere.

There exist two major generation mechanisms of oblique whistler-mode waves in the Earth's magnetosphere, such as local excitation and propagation effects (Chen et al., 2013; Gao et al., 2016; Lu et al., 2019; Mourenas

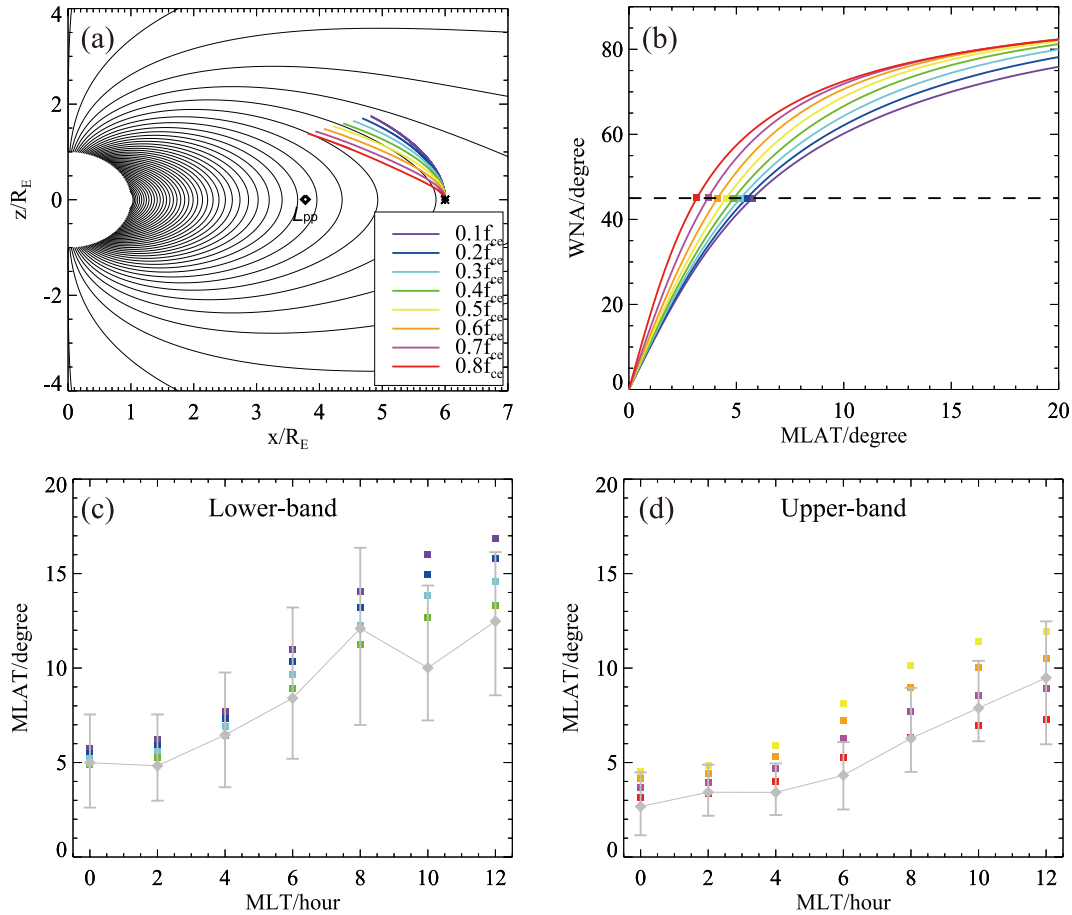

Figure 5. (a) The background magnetic field (black line) and trajectories of eight rays (color coded) at the midnight (magnetic local time [MLT] = 0 hr). (b) The wave normal angle as a function of magnetic latitude during the propagation of each whistler-mode wave. The threshold latitude of each mode is marked by square. The favored latitudes (gray diamond) of poleward propagating (c) lower-band and (d) upper-band oblique waves as a function of MLT, where the gray diamonds denote the median value with the first and third quartiles as error bars. In panel a, the plasmapause location is marked by the diamond. In panels c and d, the color coded square denotes the threshold latitude obtained from ray tracing simulations.

et al., 2015). In this study, based on the propagating direction of waves, we roughly distinguish the generation mechanism of oblique whistler-mode waves captured by Van Allen Probe-A during August 2012 to December 2018. The statistical results and ray tracing simulations suggest that the majority of oblique whistler-mode waves should be caused by propagation effects. Oblique chorus is preferentially observed away from the equator. Locally excited oblique waves are also found mainly near the equator and preferentially occur around the midnight (22–6 hr), where the energetic electrons are usually injected during substorms. This region may provide the optimal condition for locally exciting oblique whistler-mode waves, such as the anisotropic energetic electrons and beam-like electron population. Here, the beam-like electron population may be caused by the time domain structures (TDS), which are also usually observed around the midnight (Artemyev, Rankin, & Blanco, 2015; Malaspina et al., 2014; Mozer et al., 2015). It is worth noting that we cannot exclude other potential mechanisms for generation of oblique waves, such as nonlinear wave-wave coupling (Chen et al., 2017; Fu et al., 2017; Gao et al., 2017). Besides, Tsurutani et al. (2009) found the equatorward propagating oblique whistler-mode waves at $L \sim 7$ and high MLATs based on the GEOTAIL wave data (Nagano et al., 1996). Similarly, Agapitove et al. (2013) and Santolik et al. (2014) also showed that there also exist some weak oblique waves above the MLAT of 40°. However, these waves were considered to be generated in the minimum B pocket off the equator, and might not reach the range of ±20° (the concerned latitudes of this study) due to possible Landau damping.

The preferred latitudes of poleward propagating oblique whistler-mode waves are strongly dependent on MLT, which may be a consequence of the day-night asymmetry of Earth's magnetic field configuration. At midnight,

the background magnetic field is heavily stretched from the standard dipole field, then the whistler-mode wave turns oblique at very low latitude, especially for upper-band wave. These waves may damp rapidly. At noon, the whistler-mode waves become oblique at higher latitudes due to the more solar wind compressed background magnetic fields. More importantly, we find oblique whistler-mode waves seem to be confined within the low-latitude regions. For upper-band oblique waves, they have the very low occurrence rate above $\pm 15°$. For lower-band oblique waves, based on the trend shown in Figures 3c and 4c, we can estimate that lower-band oblique waves may be confined within $\pm 25°$. Therefore, if no other process is involved, after excitation at the equator, it is difficult for whistler-mode waves to reach high latitudes (>30°) since they quickly become oblique and experience severe Landau damping. However, recent studies reveal that small-scale density ducts (density peak or trough) can efficiently trap whistler-mode waves and enable them to propagate high latitudes with the small WNA (Chen, Gao, Lu, Tsurutani, Li, et al., 2021, 2021b; Ke et al., 2021). Thus, trapping of waves in density ducts may explain the existence of some high-latitude whistler-mode waves.

There already exist several statistical studies of whistler-mode waves based on Cluster data and Van Allen Probes data (Agapitov et al., 2013, 2018; Artemyev et al., 2016; Li, Santolik, et al., 2016; Santolik et al., 2014), and they have established a useful wave model for further studying the electron dynamics in the Earth's magnetosphere. However, unlike this study, they did not separate quasi-parallel and oblique waves in the statistical studies, so the clear dependence of favored MLATs on MLT (Figures 2 and 3) was not found. Besides, we also separate these waves based on their frequency and propagating direction, and find they have different generation mechanisms and source regions. We should mention that the determination of magnetic equator is not exactly accurate, and some poleward propagating waves may be selected as equatorward propagating waves. For the same reason, some equatorward propagating waves could be counted as poleward propagating waves, so the effect of inaccurate equator location should be greatly weakened in our statistical study.

Data Availability Statement

The entire Van Allen Probes data set is publicly available at https://spdf.gsfc.nasa.gov/pub/data/rbsp/. The Van Allen Probes data analysis is carried out using the publicly available SPEDAS software (http://spedas.org). The ray tracing simulation data can be accessed via https://dx.doi.org/10.12176/01.99.02673.

Acknowledgments
This research was funded by the Strategic Priority Research Program of Chinese Academy of Sciences Grant No XDB41000000, Key Research Program of Frontier Sciences CAS (QYZDJ-SSW-DQC010), the Fundamental Research Funds for the Central Universities (WK3420000013), and "USTC Tang Scholar" program. We also acknowledge the entire Van Allen Probes instrument teams.

References

Agapitov, O., Artemyev, A., Krasnoselskikh, V., Khotyaintsev, Y. V., Mourenas, D., Breuillard, H., et al. (2013). Statistics of whistler mode waves in the outer radiation belt: Cluster STAFF-SA measurements. *Journal of Geophysical Research: Space Physics*, *118*(6), 3407–3420. https://doi.org/10.1002/jgra.50312

Agapitov, O., Mourenas, D., Artemyev, A. V., Mozer, F. S., Hospodarsky, G., Bonnell, J., & Krasnoselskikh, V. (2018). Synthetic empirical chorus wave model from combined Van Allen Probes and Cluster statistics. *Journal of Geophysical Research: Space Physics*, *123*(1), 297–314. https://doi.org/10.1002/2017JA024843

Albert, J. M. (2017). Quasi-linear diffusion coefficients for highly oblique whistler mode waves. *Journal of Geophysical Research: Space Physics*, *122*(5), 5339–5354. https://doi.org/10.1002/2017JA024124

Artemyev, A., Agapitov, O., Mourenas, D., Krasnoselskikh, V., Shastun, V., & Mozer, F. (2016). Oblique whistler-mode waves in the Earth's inner magnetosphere: Energy distribution, origins, and role in radiation belt dynamics. *Space Science Reviews*, *200*(1–4), 261–355. https://doi.org/10.1007/s11214-016-0252-5

Artemyev, A. V., Agapitov, O. V., Mourenas, D., Krasnoselskikh, V. V., & Mozer, F. S. (2015). Wave energy budget analysis in the Earth's radiation belts uncovers a missing energy. *Nature Communications*, *6*(1), 8143. https://doi.org/10.1038/ncomms8143

Artemyev, A. V., Rankin, R., & Blanco, M. (2015). Electron trapping and acceleration by kinetic Alfven waves in the inner magnetosphere. *Journal of Geophysical Research: Space Physics*, *120*(12), 10305–10316. https://doi.org/10.1002/2015ja021781

Breuillard, H., Agapitov, O., Artemyev, A., Kronberg, E. A., Haaland, S. E., Daly, P. W., et al. (2015). Field-aligned chorus wave spectral power in Earth's outer radiation belt. *Annales Geophysicae*, *33*(5), 583–597. https://doi.org/10.5194/angeo-33-583-2015

Breuillard, H., Zaliznyak, Y., Krasnoselskikh, V., Agapitov, O., Artemyev, A., & Rolland, G. (2012). Chorus wave-normal statistics in the Earth's radiation belts from ray tracing technique. *Annales de Geophysique*, *30*(8), 1223–1233. https://doi.org/10.5194/angeo-30-1223-2012

Burton, R. K., & Holzer, R. E. (1974). Origin and propagation of chorus in outer magnetosphere. *Journal of Geophysical Research*, *79*(7), 1014–1023. https://doi.org/10.1029/JA079i007p01014

Carpenter, D. L., & Anderson, R. R. (1992). An ISEE/Whistler model of equatorial electron density in the magnetosphere. *Journal of Geophysical Research*, *97*(A2), 1097–1108. https://doi.org/10.1029/91ja01548

Chen, H. Y., Gao, X. L., Lu, Q. M., Ke, Y. G., & Wang, S. (2017). Lower band cascade of whistler waves excited by anisotropic hot electrons: One-dimensional PIC simulations. *Journal of Geophysical Research: Space Physics*, *122*(10), 10448–10457. https://doi.org/10.1002/2017ja024513

Chen, L., Bortnik, J., Li, W., Thorne, R. M., & Horne, R. B. (2012). Modeling the properties of plasmaspheric hiss: 1. Dependence on chorus wave emission. *Journal of Geophysical Research*, *117*(A5), A05201. https://doi.org/10.1029/2011ja017201

Chen, L. J., Thorne, R. M., Li, W., & Bortnik, J. (2013). Modeling the wave normal distribution of chorus waves. *Journal of Geophysical Research: Space Physics*, *118*(3), 1074–1088. https://doi.org/10.1029/2012ja018343

Chen, R., Gao, X. L., Lu, Q. M., Tsurutani, B. T., Li, W., Ni, B. B., & Wang, S. (2021). In situ observations of whistler-mode chorus waves guided by density ducts. *Journal of Geophysical Research*, *126*(4), e2020JA028814. https://doi.org/10.1029/2020ja028814

Chen, R., Gao, X. L., Lu, Q. M., Tsurutani, B. T., & Wang, S. (2021). Observational evidence for whistler waves guided/ducted by the inner and outer edges of the plasmapause. *Geophysical Research Letters*, *48*(6), e2021GL092652. https://doi.org/10.1029/2021gl092652

Denton, R. E., Goldstein, J., & Menietti, J. D. (2002). Field line dependence of magnetospheric electron density. *Geophysical Research Letters*, *29*(24), 2205. https://doi.org/10.1029/2002GL015963

Fu, X. R., Gary, S. P., Reeves, G. D., Winske, D., & Woodroffe, J. R. (2017). Generation of highly oblique lower band chorus via nonlinear three-wave resonance. *Geophysical Research Letters*, *44*(19), 9532–9538. https://doi.org/10.1002/2017gl074411

Gao, X. L., Chen, L. J., Li, W., Lu, Q. M., & Wang, S. (2019). Statistical results of the power gap between lower-band and upper-band chorus waves. *Geophysical Research Letters*, *46*(8), 4098–4105. https://doi.org/10.1029/2019gl082140

Gao, X. L., Chen, R., Lu, Q. M., Chen, L. J., Chen, H. Y., & Wang, X. Y. (2022). Observational evidence for the origin of repetitive chorus emissions. *Geophysical Research Letters*. (accepted).

Gao, X. L., Li, W., Thorne, R. M., Bortnik, J., Angelopoulos, V., Lu, Q. M., et al. (2014). New evidence for generation mechanisms of discrete and hiss-like whistler mode waves. *Geophysical Research Letters*, *41*(14), 4805–4811. https://doi.org/10.1002/2014gl060707

Gao, X. L., Lu, Q. M., & Wang, S. (2017). First report of resonant interactions between whistler mode waves in the Earth's magnetosphere. *Geophysical Research Letters*, *44*(11), 5269–5275. https://doi.org/10.1002/2017gl073829

Gao, X. L., Mourenas, D., Li, W., Artemyev, A. V., Lu, Q. M., Tao, X., & Wang, S. (2016). Observational evidence of generation mechanisms for very oblique lower band chorus using THEMIS waveform data. *Journal of Geophysical Research: Space Physics*, *121*(7), 6732–6748. https://doi.org/10.1002/2016ja022915

Goldstein, B. E., & Tsurutani, B. T. (1984). Wave normal directions of chorus near the equatorial source region. *Journal of Geophysical Research*, *89*(A5), 2789–2810. https://doi.org/10.1029/JA089iA05p02789

Haque, N., Spasojevic, M., Santolik, O., & Inan, U. S. (2010). Wave normal angles of magnetospheric chorus emissions observed on the Polar spacecraft. *Journal of Geophysical Research*, *115*(A4), A00f07. https://doi.org/10.1029/2009ja014717

Haselgrove, J. (1955). Ray theory and a new method for ray tracing. In *The physics of the ionosphere; report of the Physical Society Conference on the Physics of the Ionosphere* (pp. 355–364). Cavendish Lab.

Horne, R. B., Thorne, R. M., Glauert, S. A., Albert, J. M., Meredith, N. P., & Anderson, R. R. (2005). Timescale for radiation belt electron acceleration by whistler mode chorus waves. *Journal of Geophysical Research*, *110*(A3), A03225. https://doi.org/10.1029/2004ja010811

Ke, Y. G., Chen, L. J., Gao, X. L., Lu, Q. M., Wang, X. Y., Chen, R., et al. (2021). Whistler-mode waves trapped by density irregularities in the Earth's magnetosphere. *Geophysical Research Letters*, *48*(7), e2020GL092305. https://doi.org/10.1029/2020gl092305

Ke, Y. G., Gao, X. L., Lu, Q. M., Wang, X. Y., & Wang, S. (2017). Generation of rising-tone chorus in a two-dimensional mirror field by using the general curvilinear PIC code. *Journal of Geophysical Research: Space Physics*, *122*(8), 8154–8165. https://doi.org/10.1002/2017ja024178

Kessel, R. L., Fox, N. J., & Weiss, M. (2013). The radiation belt storm probes (RBSP) and space weather. *Space Science Reviews*, *179*(1–4), 531–543. https://doi.org/10.1007/s11214-012-9953-6

Kimura, I. (1966). Effects of ions on whistler-mode ray tracing. *Radio Science*, *1*(3), 269–283. https://doi.org/10.1002/rds196613269

Kletzing, C. A., Kurth, W. S., Acuna, M., MacDowall, R. J., Torbert, R. B., Averkamp, T., et al. (2013). The electric and magnetic field instrument suite and integrated science (EMFISIS) on RBSP. *Space Science Reviews*, *179*(1–4), 127–181. https://doi.org/10.1007/s11214-013-9993-6

LeDocq, M. J., Gurnett, D. A., & Hospodarsky, G. B. (1998). Chorus source locations from VLF Poynting flux measurements with the Polar spacecraft. *Geophysical Research Letters*, *25*(21), 4063–4066. https://doi.org/10.1029/1998gl900071

Li, J., Bortnik, J., An, X., Li, W., Angelopoulos, V., Thorne, R. M., et al. (2019). Origin of two-band chorus in the radiation belt of Earth. *Nature Communications*, *10*(1), 4672. https://doi.org/10.1038/s41467-019-12561-3

Li, W., Bortnik, J., Thorne, R. M., & Angelopoulos, V. (2011). Global distribution of wave amplitudes and wave normal angles of chorus waves using THEMIS wave observations. *Journal of Geophysical Research*, *116*(A12), A12205. https://doi.org/10.1029/2011ja017035

Li, W., Bortnik, J., Thorne, R. M., Cully, C. M., Chen, L., Angelopoulos, V., et al. (2013). Characteristics of the Poynting flux and wave normal vectors of whistler-mode waves observed on THEMIS. *Journal of Geophysical Research: Space Physics*, *118*(4), 1461–1471. https://doi.org/10.1002/jgra.50176

Li, W., Mourenas, D., Artemyev, A. V., Agapitov, O. V., Bortnik, J., Albert, J. M., et al. (2014). Evidence of stronger pitch angle scattering loss caused by oblique whistler-mode waves as compared with quasi-parallel waves. *Geophysical Research Letters*, *41*(17), 6063–6070. https://doi.org/10.1002/2014gl061260

Li, W., Mourenas, D., Artemyev, A. V., Bortnik, J., Thorne, R. M., Kletzing, C. A., et al. (2016). Unraveling the excitation mechanisms of highly oblique lower band chorus waves. *Geophysical Research Letters*, *43*(17), 8867–8875. https://doi.org/10.1002/2016gl070386

Li, W., Santolik, O., Bortnik, J., Thorne, R. M., Kletzing, C. A., Kurth, W. S., & Hospodarsky, G. B. (2016). New chorus wave properties near the equator from Van Allen Probes wave observations. *Geophysical Research Letters*, *43*(10), 4725–4735. https://doi.org/10.1002/2016GL068780

Liu, S., Gao, Z., Xiao, F., He, Q., Li, T., Shang, X., et al. (2021). Observation of unusual chorus elements by van allen probes. *Journal of Geophysical Research: Space Physics*, *126*(7), e2021JA029258. https://doi.org/10.1029/2021JA029258

Liu, S., Xiao, F., Yang, C., He, Y., Zhou, Q., Kletzing, C. A., et al. (2015). Van Allen Probes observations linking radiation belt electrons to chorus waves during 2014 multiple storms. *Journal of Geophysical Research: Space Physics*, *120*(2), 938–948. https://doi.org/10.1002/2014JA02078

Liu, S., Xie, Y., Zhang, S., Shang, X., Yang, C., Zhou, Q., et al. (2020). Unusual loss of Van Allen belt relativistic electrons by extremely low-frequency chorus. *Geophysical Research Letters*, *47*(18), e2020GL089994. https://doi.org/10.1029/2020GL089994

Lorentzen, K. R., Blake, J. B., Inan, U. S., & Bortnik, J. (2001). Observations of relativistic electron microbursts in association with VLF chorus. *Journal of Geophysical Research*, *106*(A4), 6017–6027. https://doi.org/10.1029/2000ja003018

Lu, Q. M., Ke, Y. G., Wang, X. Y., Liu, K. J., Gao, X. L., Chens, L. J., & Wang, S. (2019). Two-Dimensional gcPIC simulation of rising-tone chorus waves in a dipole magneitic field. *Journal of Geophysical Research: Space Physics*, *124*(6), 4157–4167. https://doi.org/10.1029/2019ja026586

Lu, Q. M., Lun, L. J., Wang, X. Y., Gao, X. L., Liu, Y., & Wang, S. (2021). Repetitive emissions of rising-tone chorus waves in the inner magnetosphere. *Geophysical Research Letters*, *48*(15), e2021GL094979. https://doi.org/10.1029/2021gl094979

Malaspina, D. M., Andersson, L., Ergun, R. E., Wygant, J. R., Bonnell, J. W., Kletzing, C., et al. (2014). Nonlinear electric field structures in the inner magnetosphere. *Geophysical Research Letters*, *41*(16), 5693–5701. https://doi.org/10.1002/2014gl061109

Mauk, B. H., Fox, N. J., Kanekal, S. G., Kessel, R. L., Sibeck, D. G., & Ukhorskiy, A. (2013). Science objectives and rationale for the radiation belt storm probes mission. *Space Science Reviews*, *179*(1–4), 3–27. https://doi.org/10.1007/s11214-012-9908-y

Mourenas, D., Artemyev, A. V., Agapitov, O. V., & Krasnoselskikh, V. (2014). Consequences of geomagnetic activity on energization and loss of radiation belt electrons by oblique chorus waves. *Journal of Geophysical Research: Space Physics*, *119*(4), 2775–2796. https://doi.org/10.1002/2013ja019674

Mourenas, D., Artemyev, A. V., Agapitov, O. V., Krasnoselskikh, V., & Mozer, F. S. (2015). Very oblique whistler generation by low-energy electron streams. *Journal of Geophysical Research: Space Physics*, *120*(5), 3665–3683. https://doi.org/10.1002/2015ja021135

Mourenas, D., Artemyev, A. V., Ripoll, J. F., Agapitov, O. V., & Krasnoselskikh, V. V. (2012). Timescales for electron quasi-linear diffusion by parallel and oblique lower-band chorus waves. *Journal of Geophysical Research*, *117*(A6), A06234. https://doi.org/10.1029/2012ja017717

Mozer, F. S., Agapitov, O. V., Artemyev, A., Drake, J. F., Krasnoselskikh, V., Lejosne, S., & Vasko, I. (2015). Time domain structures: What and where they are, what they do, and how they are made. *Geophysical Research Letters*, *42*(10), 3627–3638. https://doi.org/10.1002/2015gl063946

Nagano, I., Yagitani, S., Kojima, H., & Matsumoto, H. (1996). Analysis of wave normal and Poynting vectors of the chorus emissions observed by GEOTAIL. *Journal of Geomagnetism and Geoelectricity*, *48*(3), 299–307. https://doi.org/10.5636/jgg.48.299

Ni, B., Thorne, R. M., Shprits, Y. Y., & Bortnik, J. (2008). Resonant scattering of plasma sheet electrons by whistler-mode chorus: Contribution to diffuse auroral precipitation. *Geophysical Research Letters*, *35*(11), L11106. https://doi.org/10.1029/2008gl034032

Ni, B. B., Thorne, R. M., Meredith, N. P., Shprits, Y. Y., & Horne, R. B. (2011). Diffuse auroral scattering by whistler mode chorus waves: Dependence on wave normal angle distribution. *Journal of Geophysical Research*, *116*(A10), A10207. https://doi.org/10.1029/2011ja016517

Nunn, D. (1971). Theory of VLF emissions. *Planetary and Space Science*, *19*(9), 1141–1167. https://doi.org/10.1016/0032-0633(71)90110-3

O'Brien, T. P., & Moldwin, M. B. (2003). Empirical plasmapause models from magnetic indices. *Geophysical Research Letters*, *30*(4), 1152. https://doi.org/10.1029/2002gl016007

Omura, Y., Katoh, Y., & Summers, D. (2008). Theory and simulation of the generation of whistler-mode chorus. *Journal of Geophysical Research*, *113*(A4), A04223. https://doi.org/10.1029/2007ja012622

Santolik, O., Gurnett, D. A., Pickett, J. S., Parrot, M., & Cornilleau-Wehrlin, N. (2003). Spatio-temporal structure of storm-time chorus. *Journal of Geophysical Research*, *108*(A7), 1278. https://doi.org/10.1029/2002ja009791

Santolik, O., Macusova, E., Kolmasova, I., Cornilleau-Wehrlin, N., & de Conchy, Y. (2014). Propagation of lower-band whistler-mode waves in the outer Van Allen belt: Systematic analysis of 11 years of multi-component data from the Cluster spacecraft. *Geophysical Research Letters*, *41*(8), 2729–2737. https://doi.org/10.1002/2014gl059815

Shprits, Y. Y., & Ni, B. B. (2009). Dependence of the quasi-linear scattering rates on the wave normal distribution of chorus waves. *Journal of Geophysical Research*, *114*(A11), A11205. https://doi.org/10.1029/2009ja014223

Taubenschuss, U., Santolik, O., Breuillard, H., Li, W., & Le Contel, O. (2016). Poynting vector and wave vector directions of equatorial chorus. *Journal of Geophysical Research: Space Physics*, *121*(12), 11912–11928. https://doi.org/10.1002/2016ja023389

Thorne, R. M., Li, W., Ni, B., Ma, Q., Bortnik, J., Chen, L., et al. (2013). Rapid local acceleration of relativistic radiation-belt electrons by magnetospheric chorus. *Nature*, *504*(7480), 411–414. https://doi.org/10.1038/nature12889

Thorne, R. M., Ni, B. B., Tao, X., Horne, R. B., & Meredith, N. P. (2010). Scattering by chorus waves as the dominant cause of diffuse auroral precipitation. *Nature*, *467*(7318), 943–946. https://doi.org/10.1038/nature09467

Tsurutani, B. T., Chen, R., Gao, X., Lu, Q., Pickett, J. S., Lakhina, G. S., et al. (2020). Lower-band, "monochromatic" chorus riser subelement/wave packet observations. *Journal of Geophysical Research*, *125*(10), e2020JA028090. https://doi.org/10.1029/2020JA028090

Tsurutani, B. T., Lakhina, G. S., & Verkhoglyadova, O. P. (2013). Energetic electron (>10 keV) microburst precipitation, !5-15 s X-ray pulsations, chorus, and wave-particle interactions: A review. *Journal of Geophysical Research*, *118*(5), 1–17. https://doi.org/10.1002/jgra.50264

Tsurutani, B. T., & Smith, E. J. (1974). Postmidnight chorus - substorm phenomenon. *Journal of Geophysical Research*, *79*(1), 118–127. https://doi.org/10.1029/JA079i001p00118

Tsurutani, B. T., & Smith, E. J. (1977). 2 types of magnetospheric Elf chorus and their substorm dependences. *Journal of Geophysical Research*, *82*(32), 5112–5128. https://doi.org/10.1029/JA082i032p05112

Tsurutani, B. T., Smith, E. J., West, H. I., Jr., & Buck, R. M. (1979). Chorus, energetic electrons and magnetospheric substorms. In P. J. Palmadesso & K. Papadopoulos (Eds.), *Wave instabilities in space plasmas*, (Vol. 55–71, pp. 55–62). D. Reidel.

Tsurutani, B. T., Verkhoglyadova, O. P., Lakhina, G. S., & Yagitani, S. (2009). Properties of dayside outer zone chorus during HILDCAA events: Loss of energetic electrons. *Journal of Geophysical Research*, *114*(A3), A03207. https://doi.org/10.1029/2008JA013353

Tsyganenko, N. A. (1989). A magnetospheric magnetic field model with a warped tail current sheet. *Planetary and Space Science*, *37*(1), 5–20. https://doi.org/10.1016/0032-0633(89)90066-4

Verkhoglyadova, O. P., Tsurutani, B. T., & Lakhina, G. S. (2010). Properties of obliquely propagating chorus. *Journal of Geophysical Research*, *115*(A9), A00F19. https://doi.org/10.1029/2009JA014809

Xiao, F. L., Su, Z. P., Zheng, H. N., & Wang, S. (2009). Modeling of outer radiation belt electrons by multidimensional diffusion process. *Journal of Geophysical Research*, *114*(A3), A03201. https://doi.org/10.1029/2008ja013580

Xiao, F. L., Yang, C., Su, Z., Zhou, Q., He, Z., He, Y., et al. (2015). Wave-driven butterfly distribution of Van Allen belt relativistic electrons. *Nature Communications*, *6*(1), 8590. https://doi.org/10.1038/ncomms9590

Yagitani, S., Habagishi, T., & Omura, Y. (2014). Geotail observation of upper band and lower band chorus elements in the outer magnetosphere. *Journal of Geophysics Research Space Physics*, *119*(6), 4694–4705. https://doi.org/10.1002/2013JA019678

Zhou, Q., Xiao, F., Yang, C., Liu, S., He, Y., Wygant, J. R., et al. (2016). Evolution of chorus emissions into plasmaspheric hiss observed by Van Allen Probes. *Journal of Geophysics Research Space Physics*, *121*(5), 4518–4529. https://doi.org/10.1002/2016JA022366

Zhou, Q., Yang, C., He, Y., Liu, S., Gao, Z., & Xiao, F. (2019). Excitation of highly oblique lower band and upper band chorus by a loss cone feature and temperature anisotropy distribution. *Geophysical Research Letters*, *46*(4), 1929–1936. https://doi.org/10.1029/2018GL08137